




Critical study on the thermal-structural characteristics of worktable assembly of a dry hobbing machine

Xianguang Li¹ · Yong Yang¹ · Zheng Zou^{1,2,3}  · Zhitao Liu² · Li Wang¹ · Qian Tang²

Received: 8 February 2018 / Accepted: 10 September 2018 / Published online: 23 September 2018
© Springer-Verlag London Ltd., part of Springer Nature 2018

Abstract

Dry hobbing machine is a kind of specialized machine tool to manufacture high-quality small-module gears. With the development of shipbuilding, automobile, and wind power industries, higher request on the dry gear hobbing accuracy is called. The thermal-induced error, which accounts for 50–70% of machining error, needs to be reduced more efficiently. Hence, in-depth investigation on the thermal-structural characteristics of the dry hobbing machine is indispensable. In this paper, thermal-structural coupling numerical simulations were conducted to investigate the heat transfer process as well as thermal-induced deformation of the worktable of a YDE3120CNC gear hobbing machine in the large-volume gear production. New equations were used here to describe the convection heat transfer happened on the worktable assembly. Verifying test results proved the feasibility of the newly proposed numerical method. Following numerical simulation, results indicated that during the gear hobbing process, the highest surface temperature of the worktable assembly appeared at the top surface of the fixture, and corresponding thermal-induced deformation reached the maximum of 49.9 μm . Besides, in a large-volume production, the worktable assembly would attain thermal equilibrium in 15,000 s. Hence, the assumption widely used in previous studies on gear hobbing machines that the worktable assembly could be treated as an ideal solid without any thermal deformation is wrong. The thermal-induced deformation of the worktable assembly should be considered in the subsequent development of the thermal error compensation system.

Keywords Thermal error · Worktable assembly · Dry hobbing machine · Thermal-structural coupling analysis

Nomenclature

A	Coefficient of hob [-]	D_m	Mean diameter of bearing (mm)
b	A constant used in the calculation of the convection heat transfer coefficient [-]	F	Tangential cutting force (N)
C	A constant used in the calculation of the convection heat transfer coefficient [-]	Fr	Internal parameter [-]
C_g	Number of threads [-]	F_t	Tangential cutting force(Kgf)
C_0	Rated static bearing load (N)	f_0	Coefficient due to bearing type and lubrication method
C_w	Coefficient of workpiece material [-]	f_1	Coefficient due to bearing type and load
D	Diameter (mm)	H	Convection heat transfer coefficient [-]
		i	Groove number of hob [-]
		L	Characteristic length (m)
		M	Overall friction torque (N·m)
		M_0	Torque due to kinetic energy loss of lubricant (N·m)
		M_n	Normal modulus [-]
		M_l	Torque due to the applied load (N·m)
		N	Rotation speed (r/min)
		P_l	Internal parameter [-]
		Pr	Prandtl number [-]
		Q_B	The bearing heating, (W)
		Q_C	The cutting heat (W)
		Re	Reynolds number [-]
		S	Hob axial feed (mm/r)

✉ Zheng Zou
z.zou@cqut.edu.cn

¹ Chongqing Machine Tool (Group) Co., Ltd., Chongqing 401339, China

² The State Key Laboratory of Mechanical Transmission, Chongqing University, Chongqing 400044, China

³ College of Mechanical Engineering, Chongqing University of Technology, Chongqing 400054, China

S_n	Feed rate in axial direction (mm/r)
T	Hobbing depth(mm)
V	Air velocity (m/s)/cutting speed (m/min)
v_c	Cutting speed (r/min)
X	Coefficient of profile modification [-]
Y	Coefficient of axial load [-]
Z	Gear teeth number [-]

Greek symbols

β	Helical angle of workpiece ($^\circ$)
λ	Thermal conductivity (W/(m \cdot $^\circ$ C))
χ	Coefficient of tooth shape amendment [-]
ν_l	The kinetic viscosity of lubricant in bearings [-]
ν_a	The dynamic viscosity of air (Pa s)
ρ	Air density (kg/m 3)

1 Introduction

The dry hobbing machine is a kind of specialized machine tool to manufacture high-quality small-module gears. With the development of shipbuilding, automobile, and wind power industries, higher request on the dry gear hobbing accuracy is called. There are several factors that would influence the gear hobbing accuracy, such as thermal error, tool wear, geometrical error, and vibration.

To reduce the negative impacts of various types of machining errors on the gear hobbing accuracy, scholars have made a lot of efforts. Jiang et al. [1] developed a mathematic model to describe the gear hobbing process of a six-axis gear hobbing machine. With this application of proposed model, the geometric error of this type of gear hobbing machine was effectively controlled. On the other hand, Chiu et al. [2] proposed a new approach to adjust the eccentricity of the hob, based on which the meshing error of the hob was minimized and the tooth profile error of the production was reduced.

Similar to other types of machine tools, the thermal-induced error (thermal error for short) accounts for 60–70% of total machining error of a hobbing machine. Hence, relevant studies on gear hobbing machines were mainly concentrated on this type of machining error. To better understand the temperature distribution and consequent thermal-induced deformation in the gear hobbing, Stark et al. [3] proposed a new two-step simulation method, in which the generated heat was calculated firstly and the results were used in the following numerical simulation. Experimental data from a fly-cutting test proved the reliability of their proposed method. The thermometers are the important research tools in the experimental studies on the thermal-induced error of gear hobbing machines. Based on a comprehensive analysis of the sources of the thermal error, Guo et al. [4] reported an ICA (independent component analysis) method to reduce required number of thermometers and optimize their locations. With the help of this new method, a thermal error compensation software

system was proposed. Experiments on the Y3150K hobbing machine proved the reliability of developed thermal error compensation system. Liu et al. [5] discussed the inter-relationship between the process parameters and the hob temperature by means of experiments. The results of the discussion provided reference standards for the selecting process parameters to prolong the lives of hobs. According to the theory of Euler-Bernoulli Beam and the Kirchhoff's thin plate theory, Wang et al. [6] built the mathematical relationship between the temperature variations of key thermal points selected on the surface of hobbing machine and the thermal-induced bending deformation of the column. Based on this model, a thermal error compensation system was developed to compensate the thermal error in the x-axis direction.

It should be noted that previous-developed mathematic models of the relationship between temperature variation and thermal-induced deformation of the gear hobbing machine were established based on a hypothesis: the worktable assembly could be treated as an ideal solid without any thermal-induced deformation in the hobbing process. However, this hypothesis is in question in practice. In the gear hobbing process, the workpieces were clamped by the fixture which rotates about its own axis. As a result, theoretically, a large amount of cutting heat would transfer to the fixture and sequentially transfer to the other components of the worktable assembly. This may cause the thermal-induced deformation of the worktable assembly. Due to the deficiencies in these previously developed mathematical models, the thermal-induced deformation characteristics of the worktable assembly should be synthetically investigated. A finite element analysis is a good research method to achieve this goal.

Although few numerical studies were focused on the dry hobbing machines, many numerical analyses of other types of CNC machine tools were reported in the literature, which are useful to accurate modeling of the dry hobbing machine. Creighton et al. [7] developed a numerical model to conduct a thermal-structure coupling analysis of the spindle of a high-speed micro milling machine under different working conditions. Experiments proved the calculated temperature and deformation fields. With the help of the simulation results, a compensation system was developed to control the thermal-induced deformation of the spindle unit. Lee et al. [8] also reported a numerical study on the thermal-induced deformation of a spindle rotating at different speeds. An optimal design scheme to reduce the thermal-induced deformation of the spindle was proposed based on the simulation results. Liu et al. [9] conducted a heat-fluid-solid coupling simulation to study the thermal-induced deformation feature of a motorized spindle assembly. The correctness of the numerical simulation results was experimentally verified.

The aim of this study is to provide refined numerical model of the worktable assembly in the dry hobbing machine to discover the heat transfer process of the worktable assembly

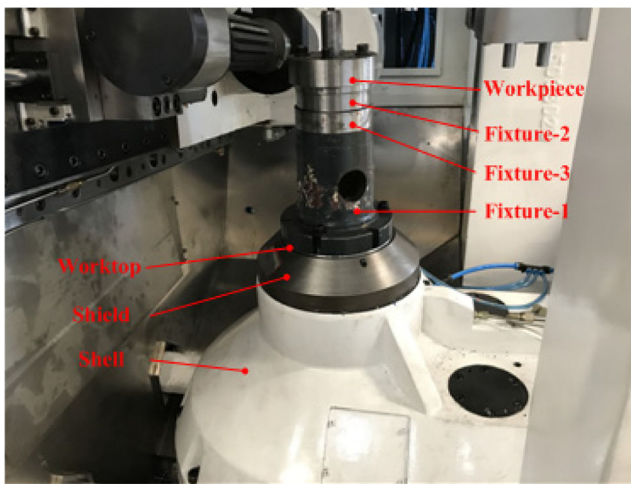


Fig. 1 The structure of the worktable assembly of the dry hobbing machine

in the cutting process, as well as both the static and transient thermal-induced deformation characteristics of the worktable assembly.

2 Modeling

2.1 Physical model

This study is based on the worktable assembly of a YDE3120CNC dry hobbing machine shown in Fig. 1. This worktable assembly mainly consists of the shell, worktop, shield, spindle, fixture, bearings, and servo motor. The typical process parameters of this gear hobbing machine and the geometric parameters of the coupled hob are listed in Table 1.

A geometric model of the worktable assembly with a simplified structure is shown in Fig. 2.

2.2 Mathematic model

For a dry gear hobbing machine in the cutting process, there are three heat sources, i. e., the friction heat of bearing, the heat generated from the servo motor, and the cutting heat. To cool the motor, the dry hobbing machine is equipped with a water chiller whose cooling capacity is significantly higher than the heat generated from the servo motor. Hence, the motor heating

was ignored in the modeling, instead, considering that the water outlet temperature of the chiller is 25 °C, the outer surface temperature of the spindle part of the motor was defined as 27 °C.

2.2.1 Quantification of cutting heat

A huge amount of heat would be released when the hob cuts the workpieces. Although both the fallen chips and compressed air ejected from the air blowers takes away a large amount of cutting heat, the rest would still transfer to the hob, workpiece, and worktable assembly. In the modeling, the cutting heat generated in the cutting process was evaluated by

$$Q_C = F_t v_C \tag{1}$$

The cutting speed was determined by:

$$v_C = \frac{\pi dn}{60} \tag{2}$$

The cutting force of the hob can be calculated according to the equation developed by Pfauter Co., Ltd. [10, 11],

$$F_t = \frac{2000m^{0.95}S^{0.8}t^{0.15}e^{0.012\beta}C_g}{v_C^{0.28}l^{0.7}A^{0.6}}e^{0.65\chi z^{-0.35}}C_w \tag{3}$$

According to the engineering experience, about 12% of the cutting heat would be left to the workpiece in the dry hobbing process. In this numerical study, the remaining heat was represented by a constant heat source placed at the outer surfaces of the workpiece. Its quantity was determined by the solution of Eqs. (1–3). By substituting the known parameters listed in Table 1 into the Eqs. (1–3), the heat load applied to the workpiece was 224.727 W.

2.2.2 Quantification of friction heat of bearings

The friction heat of bearing was evaluated by:

$$Q_B = 1.047 \times 10^{-4} M n_B \tag{4}$$

Table 1 Process parameters used in the modeling

Hobbing depth t (mm)	Hob spindle speed n_h (r/min)	hob thread number	Gear normal module m_g	Hob axial feed S (mm/r)	Outer diameter of gear hob d_h (mm)
6.75	796.18	3	3	1	80
Hob normal module m_h	Worktable spindle speed n_g (r/min)	gear tooth number	Material of workpiece	Gear helical angle β (°)	Groove number of hob i
3	59.71	40	40Cr	17.7528	14

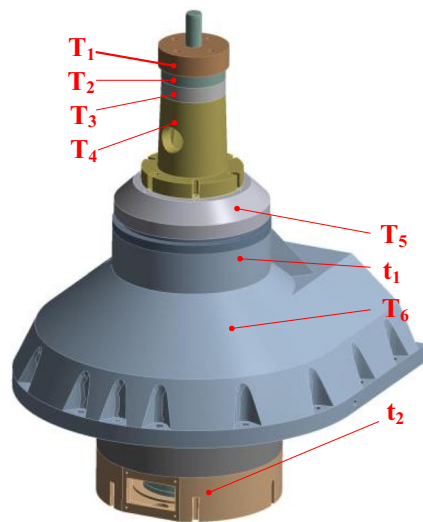


Fig. 2 The geometric model of the worktable assembly of the dry gear hobbing machine

where the overall friction torque (M) consists of two parts: the torque due to the load (M_1) and that due to the fluid kinetic energy loss (M_0). M_0 was determined by

$$M_0 = \begin{cases} 10^{-7} f_0 (v_{in})^{\frac{2}{3}} D_m^3, & v_{in} \geq 2000 \\ 160 \times 10^{-7} f_0 D_m^3, & v_{in} < 2000 \end{cases} \quad (5)$$

where the value of f_0 can be chosen from Table 2.

On the other hand, the value of M_1 can be calculated by

$$M_1 = f_1 P_1 D_m \quad (6)$$

where f_1 is the coefficient representing the bearing type and the load exerted on it, and P_1 is an internal parameter used to calculate the torque of the bearing friction. Their values can be selected from Table 3.

There are two bearings in the worktable assembly of a YDE3120CNC gear hobbing machine. One locates at the upper end of the spindle and the other is at the lower end. The friction heats generated by these bearings were defined as constant heat sources placed on the contact surfaces between the bearings and the spindle. By solving Eqs. (4–6), the

Table 2 Values of f_0 [12]

Type of bearing	Fog lubrication	Oil bath lubrication or grease lubrication
Single-row radial ball bearings	0.7~1	1.5~2
Double-row radial ball bearings	0.7~1	1.5~2
Single-row angular contact ball bearings	1	2
Double-row angular contact ball bearings	2	4

friction heats generated by these bearings were 4.38 W and 0.5 W, respectively.

2.2.3 Calculation of the forced convection heat transfer coefficient

Except for the conduction heat transfer among each components of the worktable assembly, the worktable assembly also conducts convection heat transfer with surrounding air. Therefore, accurate simulation of convection heat transfer process is key to the accuracy modeling of worktable assembly. In previous numerical studies, the forced convection heat transfer coefficient was evaluated by using an empirical equation, as shown below,

$$h = \frac{0.133 \text{Re}^{2/3} \text{Pr}^{1/3} \lambda}{L} \quad (7)$$

Although this empirical equation has been widely used in the previous studies of thermal characteristics of wet hobbing machines, it may be not fit for the case of the dry hobbing machine, which uses high-speed compressed air rather than the cooling oil to cool the cutting zone. In fact, the convection heat transfer between the worktable assembly and the compressed air is similar to the condition that air flows through a single tube. Hence, in present numerical study, another method was adopted to calculate the forced convection heat transfer coefficient, in which the convection heat transfer coefficient of the rotating surfaces was defined by the following equations:

$$h = \frac{Nu \lambda}{L} \quad (8)$$

$$Nu = C \text{Re}^b \text{Pr}^{1/3} \quad (9)$$

$$\text{Re} = \frac{\rho v L}{\nu_a} \quad (10)$$

where the values of related parameters can be selected from Table 4.

The temperature determines the thermodynamic characteristics of air. Hence, the values of thermodynamic parameters of air around the worktable assembly were derived from the average temperature between the rotating surfaces of the worktable assembly and the compressed air. In the numerical simulations, the pressure, temperature, and density of the compressed air used in the numerical simulations were 0.5 MPa, 25 °C, and 5.8455 kg/m³ respectively. Other thermodynamic properties were defined the same as those of dry air under standard atmospheric pressure [14].

According to the equations above, the calculated forced convection heat transfer coefficients of each components of

Table 3 Formulas for f_i and P_1 [13]

Type of bearing	f_i	P_1
Single-row radial ball bearings	$0.0009(P_0/C_0)^{0.55}$	$3F_a - 0.1F_r$
Double-row radial ball bearings	$0.0003(P_0/C_0)^{0.4}$	$1.4YF_a - 0.1F_r$
Single-row angular contact ball bearings	$0.0013(P_0/C_0)^{0.33}$	$F_a - 0.1F_r$
Double-row angular contact ball bearings	$0.001(P_0/C_0)^{0.33}$	$1.4F_a - 0.1F_r$

If $P_1 < F_r$, P_1 was set equal to F_r .

the worktable assembly are listed in Table 5. It should be noted that the forced convection heat transfer between the compressed air and the worktable assembly was much larger than that due to the rotating motion of the worktable assembly. Hence, only the convection heat transfer brought by compressed air was considered in the modeling.

2.2.4 Other boundary conditions

The natural convection and radiation heat transfers between the worktable assembly and surrounding air were considered in this numerical study as well. The radiation heat transfer coefficient was set at 0.82. The natural heat transfer coefficient was set as $10W/(m^2 \cdot C)$.

Besides, the shell was firmly attached to the bed of the YDE3120CNC gear hobbing machine; hence, the displacement of the shell was limited in order to accurately simulate real working conditions.

2.3 Numerical simulation procedure

The sequential coupling analysis scheme was used here to conduct both steady-state and transient-state thermo-structure coupling analysis of the worktable assembly. The steps used in the analysis conducted in this study are shown in Fig. 3.

To avoid the mesh quantity affects the prediction accuracy of our proposed model of the worktable assembly, a grid-independence test was conducted the calculation results of the same test case but with different mesh sizes (1182248, 1655162, and 2317216) were comparatively analyzed. The mean temperature of the upper surface of the fixture was used as the evaluation parameter. Three different test cases of different mesh sizes simulating the same worktable assembly were comparatively analyzed. When mesh size rose from

Table 4 The value of C and n [13]

Re	C	N
0.4~4	0.989	0.330
4~40	0.911	0.385
40~4000	0.683	0.466
4000~40,000	0.193	0.618
40,000~400,000	0.0266	0.805

1,655,162 to 2,317,216, the deviation of calculation results was smaller than 0.5%. It revealed that when the mesh size is over 1.6 millions, the solution of the numerical model would be grid independent. To save the computation resource, in following numerical investigation on the thermodynamic characteristics of the worktable assembly, the mesh with 1,655,162 elements was used and finer mesh was allocated at the fixture and the workpiece, where the cutting heat entered. The mesh of our model of the worktable assembly is shown in Fig. 4.

3 Thermal-structure coupling simulation and experimental results

3.1 The characteristics of the steady-state temperature field and thermal error

The time required to process a single workpiece and reload another was short (less than 1 min for gear hobbing and 10 s for reloading), and the process of gear hobbing was both continuous and steady. Thus, the workpiece was involved in the model of the worktable assembly, and the cutting heat left on the surfaces of the workpiece was kept constant.

Figure 5 showed the steady-state temperature distribution of the worktable assembly, in which the x-axis is parallel to the axial direction of the worktable spindle, whereas the z-axis is parallel to the axial direction of the hob. As shown in Fig. 5, the cutting heat concentrated at the workpiece, and the highest temperature (70.83 °C) appeared at the surface of the

Table 5 Calculated convection heat transfer coefficients of each components of the worktable assembly

Part	Coefficient of forced convection heat transfer ($W/m^2 \cdot C$)
Workpiece	159.12
The end of fixture1	5.70
The center of fixture 1	5.42
The end of fixture 2	5.48
The center of fixture 2	5.87
Fixture 3	5.48

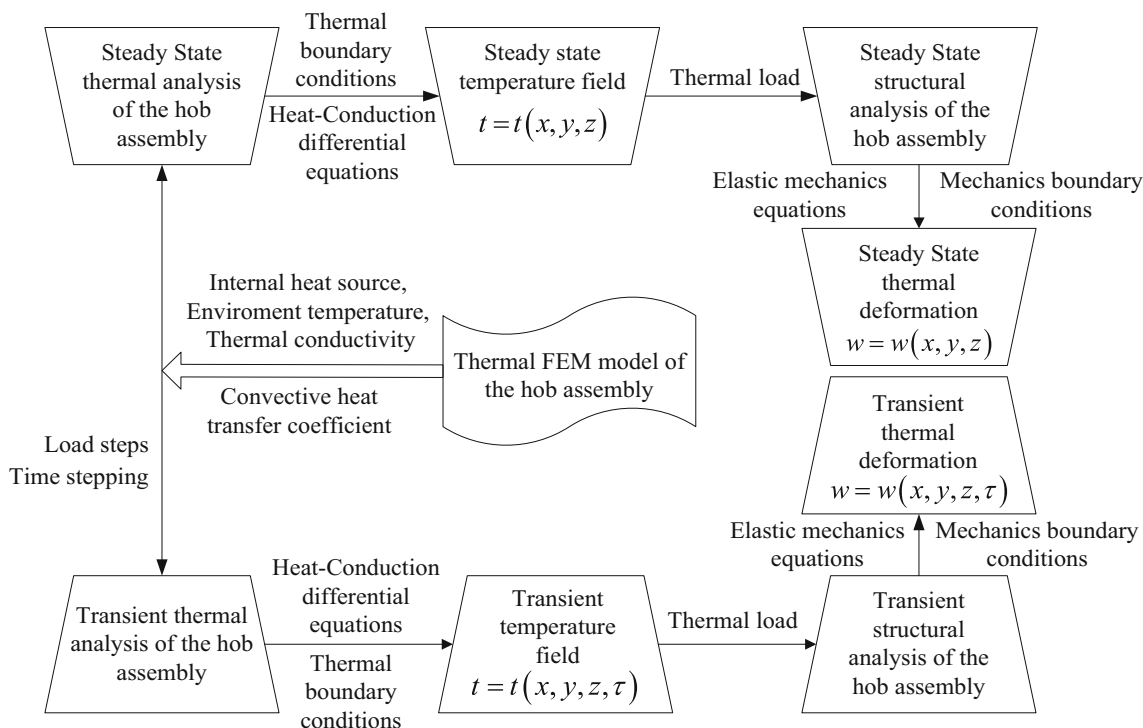


Fig. 3 Thermal-structural coupling finite element analysis

workpiece. The temperature of the worktable assembly decreases from the top to the bottom along the axial direction, reaching its lowest at the base shell (25.24 °C). This temperature was only slightly higher than the temperature of compressed air. It is possible because although a part of cutting heat transfers to the worktable assembly by heat conduction, most of it still remained at the workpiece, which caused the highest temperature to appear at the surface of the workpiece. On the other hand, due to the long heat transfer distance and large exposed area to surrounding air, the temperature of the

shell at the bottom of the worktable assembly had the lowest temperature.

Based on the obtained temperature field of the worktable assembly, analyses of structural deformation in three axis-directions were carried out as well. The thermal-induced deformation fields in the x-, y-, and z-directions are shown in Fig. 6, respectively. Figure 6a revealed that the largest total thermal-induced deformation of the worktable assembly appears at the fixture (49.88 μm). The explanation for this observation is that the upper end of the fixture directly contacted the workpiece where the cutting heat enters, whereas its opposite end was close to the base shell, which had lowest

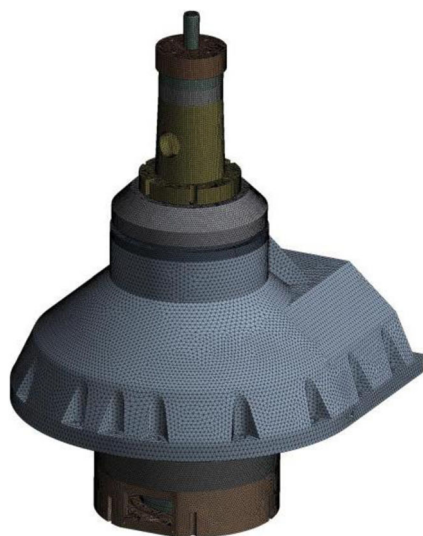


Fig. 4 The mesh of the developed model of the worktable assembly

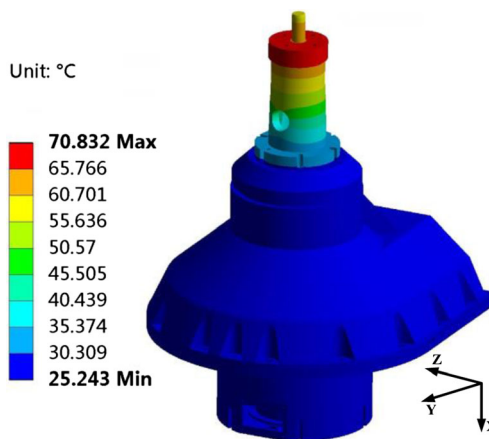
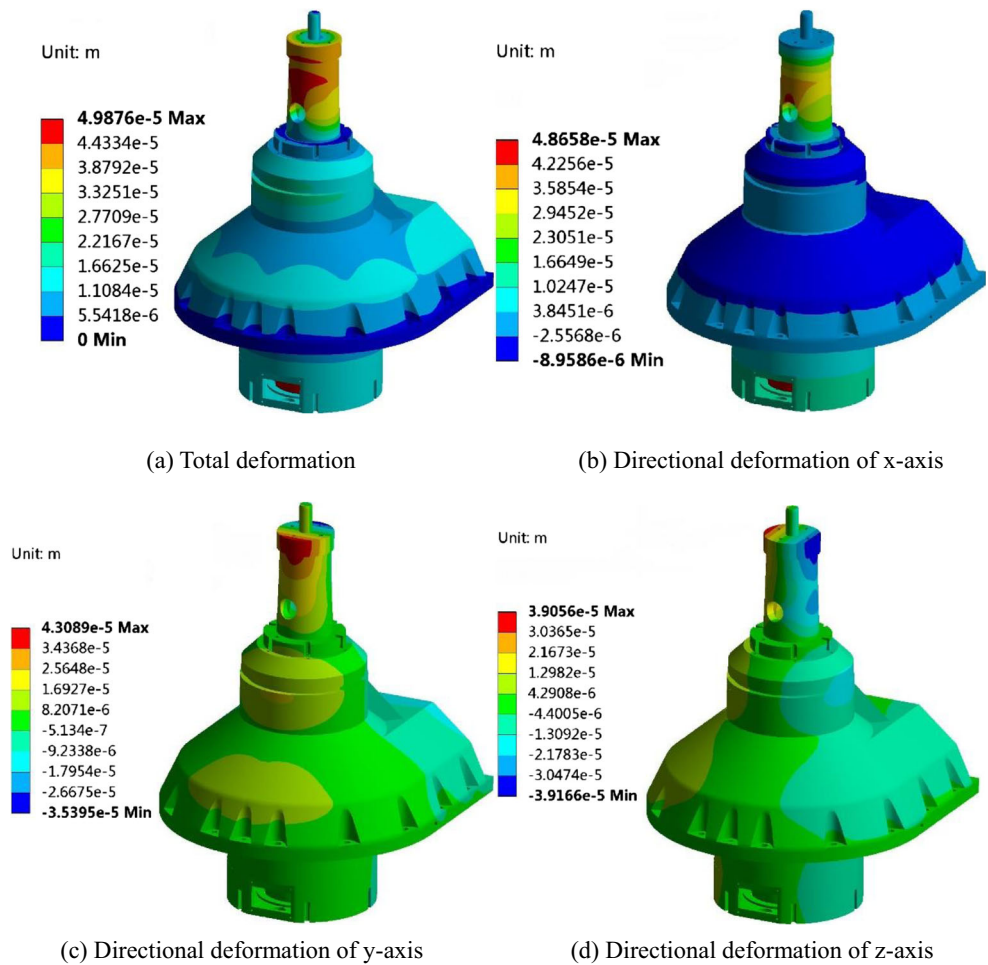


Fig. 5 Steady temperature field of the worktable assembly

Fig. 6 Steady thermal-induced deformation fields of the worktable assembly



temperatures in the cutting process. This temperature difference between the two ends of the fixture causes the largest

temperature gradient, leading to the largest thermal-induced deformation.

Fig. 7 Temperatures of the key points increased over time

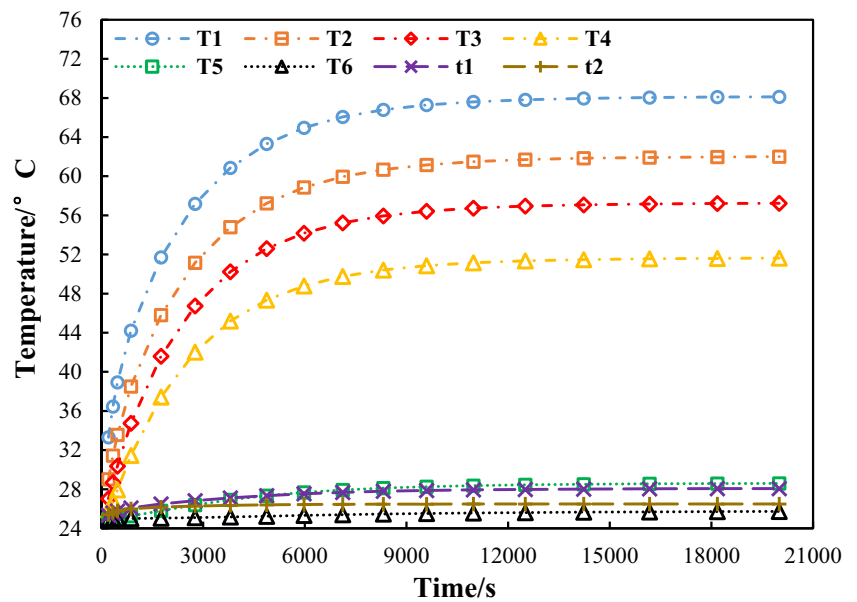


Table 6 The locations of eight key points

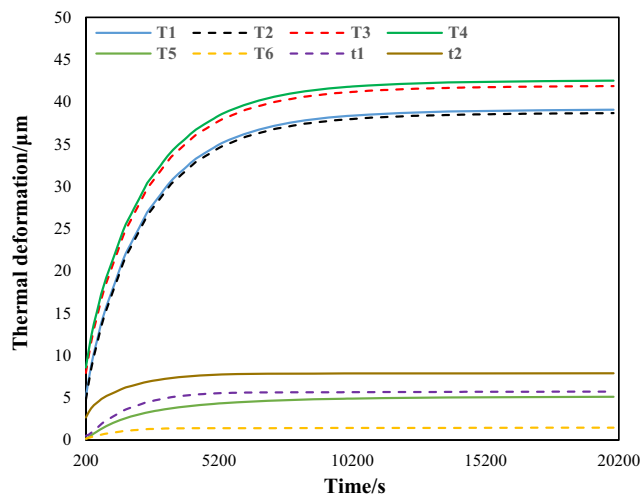
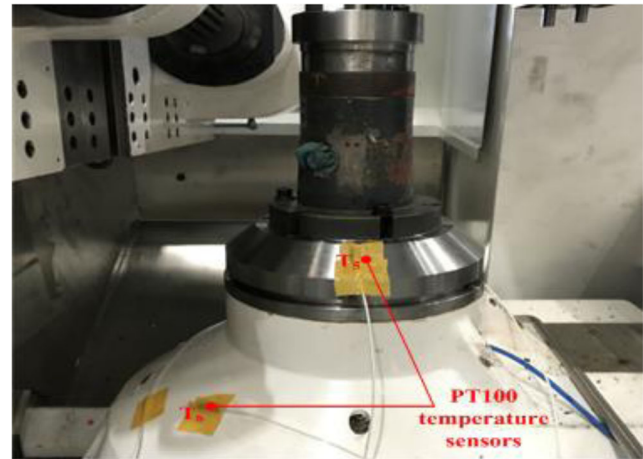
Key points	Location
T_1	Outer surface of the workpiece
T_2	Outer surface of the fixture2
T_3	Outer surface of the fixture3
T_4	Outer surface of the fixture1
T_5	Outer surface of the shield
T_6	Outer surface of the shell
t_1	Bearings at the upper end of spindle
t_2	Bearings at the lower end of spindle

Because the thermal-induced deformation in the y-axis direction was the most important effect factor of the tooth profile error in gear hobbing, it was necessary to find out which component is the most vulnerable to the y-axis-direction deformation. As shown in Fig. 6b, the largest y-axis-direction deformation appeared at the workpiece, which was $43.09 \mu\text{m}$. The reason is that the workpiece was fixed by the fixture and the center above it, which limited the displacement in the axial direction. Therefore, the thermal-induced deformation has to happen at other directions.

3.2 The characteristics of the time-variant temperature distribution and the thermal error

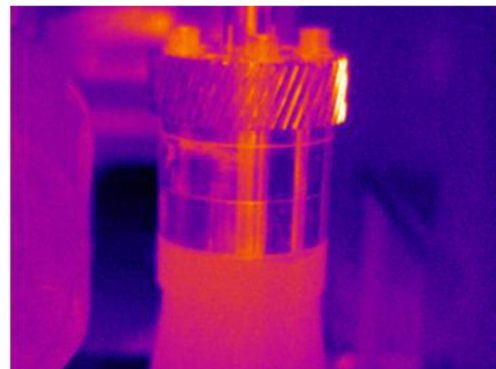
To further comprehend how the temperature and deformation fields vary with time, the transient-state thermal-structure characteristics of the worktable assembly were analyzed as well. Eight points from the surface of the worktable assembly were selected and monitored. Figure 2 and Table 6 show the locations of these eight points.

As shown in Fig. 7, temperature of these eight points varies with time and location: the closer to the workpiece, the faster

**Fig. 8** Deformation trend of then monitoring points**Fig. 9** The locations of PT100 thermometers used in the experiments

the temperature rises. At the initial stage of large-volume gear hobbing, the temperature of the worktable assembly kept increasing and subsequently leveled off. It is because that the compressed air cools the worktable assembly by the convection heat transfer. The heat transfer rate mainly depends on the difference between the air temperature and surface temperature of each component. At the initial stage of large-volume gear hobbing, the cutting heat accumulated on the worktable assembly was relatively small. Therefore, the surface temperature of the worktable assembly was close to surrounding air temperature, which led to the less heat dissipated therefore the quick rise in the surface temperature of the worktable assembly. As the increasing of heat accumulated on the worktable assembly, the increasing temperature disparity between the worktable assembly and the surrounding air caused an increase in the heat transfer rate. At the later stage of large-volume dry gear hobbing, the cutting heat inputted and the heat dissipated finally reached equilibrium (Table 6). Figure 7 also revealed that the thermal balance of the worktable assembly can be found in 15,000 s.

Figure 8 shows the tendencies of thermal-induced deformations at these eight monitoring points. No matter at

**Fig. 10** A thermal image taken in the experiment

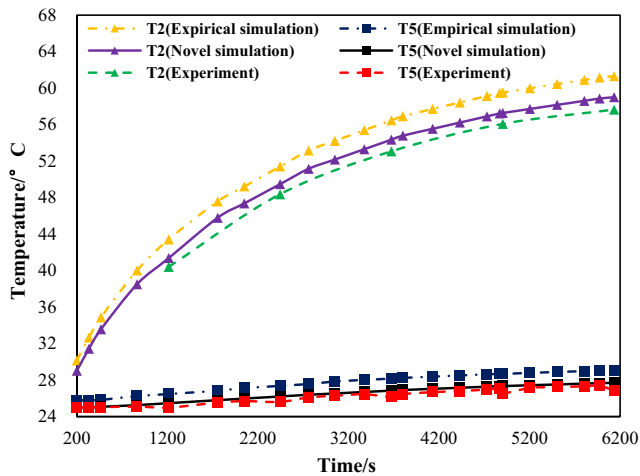


Fig. 11 Change tendencies of the temperature at the points of T2 and T5

which points, the magnitude of thermal-induced deformation increased rapidly in the first 2 h. After that, the deformation velocity of these points gradually decreased and finally, no further deformation happened. Besides, although there was a similarity between the change tendencies of temperatures and those of deformations at these eight points, the deformation magnitudes of these points were not necessarily dependent on their temperatures. Take T_1 as an example, the point T_1 had the highest temperature in later stage of the gear hobbing process (68.12 °C), but the amount of deformation was relatively small (39.7 μm). An explanation for this finding is that the deformation magnitude was more associated with temperature gradient than the temperature itself.

3.3 Experimental verification

To prove the reliability of the developed thermal-structure coupling analysis model, an experimental test was run. In this experiment, the working condition of the dry hobbing machine was the same as those listed in Table 1. Two

temperature sensors (PT100) were used to measure the outer surface temperature of the shell in the worktable assembly (T5, T6), and a thermal infrared imager (Ti400) was adopted to measure the temperatures of T1-T4 located at the rotating components of the worktable assembly. Figure 9 shows the locations of the temperature sensors placed at the shell.

One hundred gears were processed in the experiments, which took 6000 s in total. The whole gear hobbing process was automatically stopped at regular intervals, i. e., 30 s in every 1,200 s. In each interval, the temperatures of the points T1-T4 were measured by the infrared imager. A thermal image taken in the test is shown in Fig. 10. On the other hand, temperatures at the points T1-T4 were monitored in real-time during the experiment.

As revealed in Fig. 11, in the transient-state temperature field analysis of the worktable assembly, calculated temperatures of T1-T6 were relatively higher than the experimental data, and there was a deviation between the experimental curve and the curve derived from the numerical simulation results. This is because that in each intervals of the experiment, the shield of the dry hobbing machine must be opened in order to measure the temperatures of T1-T4. In this case, there was an exchange between the warmer air inside and cooler ambient air outside of the dry hobbing machine. Hence, more heat was taken away from the worktable assembly by the convection heat transfer. However, as suggested by Table 7, the relative error between experiment data and simulation results was only 5%; the accuracy of our proposed numerical model was acceptable. Figure 11 also indicated that the numerical simulation results achieved by using Eq. (7) had a larger deviation from the experimental curve than those obtained by using Eqs. (8–10). It verified our point that the set of Eqs. (8–10) is fitter for the simulation of the forced convection heat transfer that happens to the worktable assembly.

The satisfactory agreement between the calculated results and the experimental data indicates that the newly

Table 7 Comparison between the simulation results and the experimental data

No. of the critical temperature measuring points	T_2		T_5		T_6	
	Initial temperature	Final temperature	Initial temperature	Final temperature	Initial temperature	Final temperature
Experimental values (°C)	40.41	57.65	25.01	26.85	25.00	25.02
Simulation values from novel method (°C)	41.38	59.02	25.02	27.71	25.00	25.33
Relative error (%)	2.40	2.38	0.04	3.20	0	1.24
Simulation values from empirical method (°C)	43.42	61.32	25.77	29.05	25.51	27.30
Relative error (%)	7.47	6.37	3.05	8.21	2.03	9.14

proposed numerical model is a good research tool to investigate the thermal behavior of the worktable assembly. Furthermore, this model is very helpful in the optimization design of the worktable assembly.

4 Conclusions

To comprehend the thermal-structural characteristics of the worktable assembly of the dry gear hobbing machine, a precise model was developed in this study. Its accuracy was experimentally verified lately. According to the experimental data and numerical simulation results, the following conclusions were received:

1. The convection heat transfer occurs to the worktable assembly can be analogous to the condition that air flows through a single tube. Therefore the equations corresponding to this situation is fitter for the modeling of the worktable assembly.
2. In the large-volume gear hobbing process, the temperature at the workpiece was highest at all, whereas the temperature of the shell at the bottom of the worktable assembly was lowest (25.24 °C). Besides, the largest thermal-induced deformation appears at the fixture (49.9 μm). Hence, the previous assumption that the worktable assembly could be treated as an ideal solid without any thermal-induced deformation is wrong.
3. The temperature of worktable assembly rose sharply in the first 2 h of large-volume gear hobbing process. However, the worktable assembly reached the thermal equilibrium in 5 h.

Funding information This study was supported by the Chongqing Outstanding Youth Scholar Special Foundation (cstc2014jcyj70001), the China Postdoctoral Science Special Foundation (2017M612920), the Key Program of National Natural Foundation of China (51635003), the Chongqing Postdoctoral Science Special Foundation (Xm2017044, Xm2017110), and the Chongqing Scientific and Technological Innovation Leader Project.

Publisher's Note Springer Nature remains neutral with regard to jurisdictional claims in published maps and institutional affiliations.

References

1. Jiang J, Fang Z (2015) High-order tooth flank correction for a helical gear on a six-axis CNC hob machine. *Mech Mach Theory* 91:227–237
2. Chiu H, Umezaki Y, Ariura Y (1989) An improvement of the tooth profile accuracy of a hobbed gear by adjusting the hob eccentricity. *JSME Int J* 32(1):131–135
3. Stark S, Beutner M, Lorenz F, Uhlmann S, Karpuschewski B, Halle T (2013) Heat flux and temperature distribution in gear hobbing operations. *Procedia Cirp* 8:456–461
4. Guo Q, Yang J, Wang X (2007) Thermal error analysis and modeling for error compensation on gear hobbing machine. *Vacuum Sci Technol*:343–349
5. Dawei L, Zhimin B, Guo H (1999) Study on the cutting temperature in gear hobbing. *Chin J Mech Eng* 12(2):142–147
6. Wang S, Yang Y, Li X, Zhou J, Kang L (2013) Research on thermal deformation of large-scale computer numerical control gear hobbing machines. *J Mech Sci Technol* 27(5):1393–1405
7. Creighton E, Honegger A, Tulsian A, Mukhopadhyay D (2010) Analysis of thermal errors in a high-speed micro-milling spindle. *Int J Mach Tools Manuf* 50(4):386–393
8. Lee J, Kim D, Lee C (2015) A study on the thermal characteristics and experiments of high-speed spindle for machine tools. *Int J Precis Eng Manuf* 16(2):293–299
9. Liu T, Gao W, Zhang D, Zhang Y, Chang W, Liang C, Tian Y (2017) Analytical modeling for thermal errors of motorized spindle unit. *Int J Mach Tool Manu* 112:53–70
10. Chen P (2002) Research and application of virtual prototype-based design for CNC gear hobbing machine. In: Master thesis. Chongqing University, China
11. Yu C, Huang X (2007) Analysis of calculating methods for hobbing force. *Tool Engineering* 41(3):42–45
12. Wan C (1987) Analysis method of rolling bearing. China Machine Press, Beijing
13. Holman J P (1997) Heat transfer. 8th ed. New York: McGraw – Hill Companies, 289, 305, 364
14. Kroger DG (2004) Air-cooled heat exchanger and cooling towers. Penwell Corp, Tulsa